



# Modeling dissolved inorganic carbon considering submerged aquatic vegetation

Nakayama, K. ; Komai, K. ; Tada, K. ; Lin, H. C. ; Yajima, H. ; Yano, S. ; Hipse, M. R. ; Tsai, J. W.

---

**(Citation)**

Ecological Modelling, 431:109188

**(Issue Date)**

2020-09-01

**(Resource Type)**

journal article

**(Version)**

Accepted Manuscript

**(Rights)**

© 2020 Elsevier B.V.

This manuscript version is made available under the CC-BY-NC-ND 4.0 license  
<http://creativecommons.org/licenses/by-nc-nd/4.0/>

**(URL)**

<https://hdl.handle.net/20.500.14094/90007400>



1  
2  
3  
4 **Modelling dissolved inorganic carbon considering submerged aquatic vegetation**

5  
6 K Nakayama<sup>1</sup> K Komai<sup>2</sup> K Tada<sup>3</sup> HC Lin<sup>1</sup> H Yajima<sup>4</sup> S Yano<sup>5</sup> MR Hipsey<sup>6</sup> JW Tsai<sup>7</sup>

7  
8 *1 Graduate School of Engineering, Kobe University, 1-1 Rokkodai-cho Nada-ku, Kobe*  
9 *city, 658-8501, Japan*

10 *2 School of Earth, Energy and Environmental Engineering, Kitami Institute of Technology*  
11 *165 Koen-cho Kitami, 090-8507, Japan*

12 *3 Chuden Engineering Consultants, 2-3-30 Deshio, Minami-ku, Hiroshima 734-8510,*  
13 *Japan Japan*

14 *4 Estuary Research Center, Shimane University, 1060 Nishikawatsu-cho, Matsue city,*  
15 *690-8504, Japan*

16 *5 Graduate School of Engineering, Kyushu University, 744 Moto-oka Nishi-ku, Fukuoka*  
17 *819-0395, Japan*

18 *6 Aquatic Ecodynamics, UWA School of Agriculture and Environment, The University of*  
19 *Western Australia, Australia*

20 *7 Department of Biological Science and Technology, China Medical University, Taiwan*

21  
22 *Corresponding author: K Nakayama*

23 *Tel: +81788036056*

24 *E-mail: nakayama@phoenix.kobe-u.ac.jp*

25 *Address: Graduate School of Engineering, Kobe University, 1-1 Rokkodai-cho*  
26 *Nada-ku, Kobe city, 658-8501, Japan*

27

28

29 **Highlights**

- 30 ● Aquatic vegetation can contribute to carbon capture in a lagoon system.
- 31 ● A Seasonal NEP (SNEP) model is presented to estimate the change in DIC.
- 32 ● The model can be applied to estimate lagoon productivity with limited  
33 information.
- 34 ● Model results highlight the importance of estimating residence time.
- 35 ● The SNEP model proves benefit of seagrass restoration on effective carbon  
36 capture.
- 37

38 **ABSTRACT:**

39 Net absorption of CO<sub>2</sub> by vegetated coastal ecosystems has been revealed as a key mechanism  
40 to capture and store carbon via the renewal of epigeal stem and rhizome biomass. Submerged  
41 aquatic ecosystems, such as seagrass meadows, have been termed “blue carbon” ecosystems  
42 because they absorb CO<sub>2</sub> for their underwater growth. Irradiance and water temperature are  
43 significant factors controlling net ecological production (NEP) by seagrass. As seagrass tends to  
44 grow in calm coastal areas subject to water-column stratification, such as lagoons, a new method  
45 for evaluating NEP accurately to assess blue carbon capture in these enclosed waters is required.  
46 This study aimed to develop a model to investigate thermal effects, considering irradiance, on  
47 changes in dissolved inorganic carbon dynamics in a lagoon system, and assessment of the model  
48 to understand controls on carbon dynamics in Komuke Lagoon, Japan. NEP was successfully  
49 modelled by verifying its robustness against field observations. Furthermore, the proposed model  
50 can be applied to assess and enhance the effectiveness of blue carbon capture and storage as part  
51 revegetation measures to mitigate against global warming.

52

53 **Keywords:** photosynthesis; respiration; net ecosystem production; lagoon;  
54 macrophyte

55

56

57 1. Introduction

58 Urgent adaptation and mitigation measures are required to address natural disasters, such as  
59 floods, droughts, extreme heat, and landslides, which have been increasing due to global warming  
60 (IPCC, 2014). Such action depends on effective adaptation and mitigation measures. Vegetated  
61 shallow regions have recently been revealed to absorb and capture carbon dioxide by submerged  
62 aquatic vegetation - a potential sink of anthropogenic carbon, termed “blue carbon” (Duarte et al.,  
63 2013). Nellmann (2009) showed the effectiveness of the net absorption of CO<sub>2</sub> by blue carbon  
64 ecosystems, and it has been demonstrated that about 55 % of the carbon fixed by photosynthetic  
65 activity on the Earth is in the form of blue carbon. Seagrass beds or meadows capture and store  
66 autochthonous carbon from primary production and allochthonous carbon loaded from other areas  
67 during the renewal of their epigeal stem and rhizome biomass (Kennedy et al., 2010; Fourqurean  
68 et al., 2012). Therefore, there is the possibility that CO<sub>2</sub> is captured and stored in large amounts  
69 in shallow water areas dominated by submerged aquatic vegetation (Macreadie et al, 2019). For  
70 example, Beer et al. (1997) demonstrated that eelgrass plays a great role in carbon fixation and  
71 Palacios et al. (2007) also demonstrated that seagrass meadows can be absorb CO<sub>2</sub> from the  
72 atmosphere. However, Short (1999) indicated the difficulty in predicting the impact of global  
73 climate change effects on seagrass communities, as it remains unclear how photosynthesis and  
74 the productivity of aquatic plants will react to changes in the physical conditions of aquatic  
75 ecosystems under a changing environment. Tada et al. (2018) demonstrated the potential for  
76 application of a three-dimensional hydrodynamic model to evaluate the release and absorption of  
77 CO<sub>2</sub> by eelgrass (*Zostera marina*) in Komuke Lagoon of Hokkaido Island in Japan (Shintani and  
78 Nakayama, 2010; Nakayama et al., 2012; Nakayama et al., 2014; Nakayama et al., 2016;  
79 Nakayama et al., 2019). In this study, an attempt was made to model Dissolved Inorganic Carbon  
80 (DIC) by simulating the effect of respiration and photosynthesis by eelgrass, where the CO<sub>2</sub>  
81 concentrations were estimated from DIC, Total Alkalinity (TA), water temperature and salinity  
82 by assuming a chemical equilibrium state (per Zeebe et al., 2001). As a result, while DIC in this  
83 lagoon varied in the range 300 μmol-C kg<sup>-1</sup> to 1300 μmol-C kg<sup>-1</sup>, photosynthesis was found to  
84 exceed respiration, which resulted in an estimated sink for DIC of 325 μmol-C kg<sup>-1</sup> (Tada et al.,  
85 2018). Additionally, Tada et al. (2018) showed that the influence of water temperature on  
86 photosynthesis and respiration should be included in numerical models of DIC dynamics due to  
87 its significance controlling eelgrass productivity.

88 Growth due to photosynthesis in eelgrass has been investigated in many previous studies based  
89 on photon flux density (often termed “photosynthetically active irradiance”, PAR) estimates (see

90 review by Lee et al., 2007). A Jassby type equation was found to fit to growth rates in laboratory  
91 and field experiments (Drew et al., 1979; Goodman et al., 1995; Holmer et al., 2001; Marsh et al.,  
92 1986; Olesen et al., 1993; Touchette, 1999; Zimmerman et al., 1995; Zimmerman et al., 1997).  
93 However, the best model resolving DIC changes in relation to photon flux density remains  
94 unresolved. For investigating the effect of eelgrass photosynthesis on DIC dynamics, it is  
95 necessary to measure daily changes in photon flux density, since DIC decreases greatly due to  
96 photosynthesis during the daytime with a smaller increase in DIC due to respiration during the  
97 night. Therefore, the duration of photon flux density has been shown to be more important than  
98 the light compensation point and light saturation point in evaluating eelgrass production rates  
99 (Dennison et al., 1982; Dennison et al., 1985). Additionally, Tada et al. (2018) revealed that  
100 accurate topography must also be resolved for evaluating variability in DIC, based on predictions  
101 using a three-dimensional hydrodynamic model. Overall, spatial distributions in underwater  
102 photon flux density, nutrients, turbidity, and physical conditions have all been revealed to  
103 contribute strongly to the net growth of eelgrass (Dennison et al., 1986). Beyond depth as a  
104 primary determinant of growth, turbidity plays a great role in the photosynthesis of submerged  
105 aquatic vegetation, as it increases light attenuation and reduces the photon flux density, which  
106 results in suppression of the growth of eelgrass (Dennison, 1987; Moore et al., 1997). This  
107 turbidity effect on productivity could be due to the effect of algal blooms reducing the effective  
108 underwater photon flux density due to a high water column light extinction rate (Borum, 1985),  
109 or due to excessive sediments brought about from inflows or resuspension (Adams et al., 2016).  
110 Therefore, it is necessary to develop a DIC model which can resolve changes in photon flux  
111 density precisely from the viewpoint of the suppression of photon flux density due to high  
112 turbidity or algae blooms.

113 The effect of eelgrass photosynthesis on DIC has been shown to create site-specific patterns. For  
114 example, in previous studies, the minimum light requirement has been investigated, showing large  
115 variability from 5 % to about 40 % of the maximum irradiance (Dennison et al., 1993; Koch et al.,  
116 1996; Olesen et al., 1993). Additionally, the optimal growth temperature of eelgrass has been  
117 shown to range broadly from 13 °C to 24 °C in temperate zones (Boström et al., 2004; Ibarra-  
118 Obando et al., 1987; Lee et al., 2005; Lee et al., 2006; Moore et al., 1996; Sand-Jensen, 1975;  
119 Sfriso et al., 1998; Watanabe et al., 2005). In tropical or subtropical zones, the optimal growth  
120 temperature of eelgrass has been shown to range from 16 °C to 30 °C (Biebl et al., 1971; Cabello-  
121 Pasini et al., 2003; Dennison, 1987; Drew, 1979; Evans et al., 1986; Marsh et al., 1986; Penhale,  
122 1977). Therefore, it is necessary to model the effects of eelgrass photosynthesis and respiration

123 on DIC dynamics in order to reflect regional characteristics under different climates.

124 Related to respiration and photosynthesis of eelgrass, it has been revealed that seagrass growth  
125 and production can be limited by nutrients even though photon flux density is plentiful (Coleman  
126 et al., 1994; Dennison et al., 1987; Iizumi and Hattori, 1982; Murray et al., 1992; Orth, 1977;  
127 Orth et al., 1983; Short et al., 1995; Thursby et al., 1982; Van Lent et al., 1995; Williams et al.,  
128 1993). There are many studies that have related the growth rate of eelgrass to nutrient supply from  
129 the roots (Boström et al., 2004; Dennison et al., 1987; Iizumi et al., 1982; Jørgensen, 1982;  
130 Mazzella et al., 1986; Moore et al., 1996; Pedersen et al., 1993; Short, 1987). The contribution of  
131 sediment nutrients to eelgrass growth rates has been found to be equal or be more than that from  
132 the water column (Short et al., 1984; Pedersen et al., 1992). Furthermore, Capone (1982) showed  
133 that nutrient concentrations vary greatly due to the presence of eelgrass, and nutrient pools have  
134 been shown to have rapid turnover rates. However, Burkholder et al. (1992, 1994) demonstrated  
135 that high nutrient enrichment inhibited eelgrass growth due to carbon limitation, phosphorus  
136 limitation, or other internal nutrient imbalances leading to physiological effects (Burkholder et  
137 al., 1992; Burkholder et al., 1994). Zimmerman et al. (1987) demonstrated the application of a  
138 numerical model to evaluate how nutrients affect the ecological functions of eelgrass, including  
139 respiration and photosynthesis. Therefore, in the context of nutrient supply, it can again be said  
140 that it is necessary to develop a detailed and precise submerged aquatic vegetation model for  
141 evaluating CO<sub>2</sub> flux.

142 Aside from light, photosynthesis parameters change seasonally due to differences in growth  
143 rate and water temperatures (Dennison, 1987; Orth et al., 1986; Phillips et al., 1983), with water  
144 temperature considered the primary factor controlling seasonal growth (Bulthuis, 1987; Setchell,  
145 1929). Martin et al. (2006) showed that net CO<sub>2</sub> flux increases with the seasonal increase in water  
146 temperatures in the Bay of Brest, Western Brittany, France, with similar patterns in net O<sub>2</sub> flux.  
147 However, very limited studies have investigated how this temperature variability affects DIC  
148 fluxes. As submerged aquatic vegetation tends to grow best in calm, stratified coastal areas such  
149 as enclosed bays and lagoons, methods resolving the interaction between hydrodynamics,  
150 vegetation and carbon are required for application to these types of ecosystems. Therefore, this  
151 study aims to investigate thermal effects, considering irradiance, on changes in DIC fluxes under  
152 nutrient-rich (non-limiting) conditions. We develop a simplified and practical model to  
153 understand DIC dynamics, based on easily measurable experimental data, that can be applied to  
154 estimate seasonal productivity. The model is verified through application to Komuke Lagoon,  
155 Japan, where it is used to estimate carbon uptake by eelgrass.

156

## 157 2. Method

### 158 2.1. Laboratory experiments

159 Komuke Lagoon is connected to the Sea of Okhotsk through a tidal inlet and has a volume of  
160 approximately 3,333,000 m<sup>3</sup> and a maximum water depth of 3 m (Fig. 1). Although the tidal range  
161 of the Sea of Okhotsk is approximately 1 m, the tidal range of Komuke Lagoon is only 0.5 m  
162 because of the narrow 15 m width of the tidal inlet. For this reason, calm water conditions are  
163 usual in Komuke Lagoon and the eelgrass population is widely distributed. A laboratory  
164 experiment evaluating photosynthesis was conducted with lagoon water and eelgrass collected on  
165 the 25<sup>th</sup> of June 2018 at the sampling point (44° 15' 7.3" E, 143° 30' 38.9" N) shown in Fig.  
166 1. The experiment was conducted outdoors in fine weather using a transparent acrylic water tank  
167 with a depth of 150 cm, a width of 20 cm, and a length of 20 cm (Fig. 2). Four shoots of eelgrasses  
168 taken from the lagoon were deployed in the water tank. The roots of the eelgrass were covered  
169 with vinyl sheets to avoid oxygen consumption by oxygen-demanding substances contained in  
170 the sediment. The salinity of the water used in the experiment was 22 psu. The dimensions (leaf  
171 width, length, and thickness) of eelgrass used in experiment were measured before  
172 experimentation (Table 1).

173 Two thermometers (Eijkelkamp Co. Ltd., SERA Diver) and two light quantum loggers (JFE  
174 Advantec Co. Ltd., DEFI2-L) were deployed in the water tank, recording every ten minutes. The  
175 experiment started at night, when photosynthesis was inactive, and continued for twenty-four  
176 hours. To provide vertically uniform conditions for eelgrass in the water tank, the water was well  
177 mixed using a peristaltic pump with a flow rate of 7 mL min<sup>-1</sup> through a silicon tube with a diameter  
178 of 2 mm; the water was gently taken from an inlet at a height of 100 cm from the tank bottom  
179 through the silicon tube and discharged from an outlet at a height of 0 cm from the tank bottom.  
180 The uniformity of water quality profiles in the water tank was confirmed by measuring  
181 temperatures periodically.

182 Approximately 200 mL water samples were taken from the water tank into a Scott Duran bottle  
183 by syringe and tube apparatus every hour. After sampling, 200 µL of a saturated aqueous solution  
184 of mercuric chloride was quickly added to the sample to prevent biological activity. DIC and TA  
185 of the water sample was then measured using a Total Alkalinity meter (Kimoto Electronic Co.  
186 Ltd., ATT-15) within 2 hours of sampling. Titrant for volumetric analysis (Kanto Kagaku, Co.  
187 Ltd., 0.1 mol L<sup>-1</sup> hydrochloric acid) was used for DIC and TA measurement by high accuracy  
188 titration. Additionally, a water tank experiment under the same conditions but without eelgrass



189 was conducted as a control experiment. Concentrations of NO<sub>3</sub>-N, NO<sub>2</sub>-N, NH<sub>4</sub>-N, and PO<sub>4</sub>-P in  
 190 water samples were measured for each experiment using an auto-analyzer (BLTEC Co. Ltd.,  
 191 QuAAtro 2HR).

192 The wet weight, dry weight, and carbon content of four eelgrass used in the laboratory  
 193 experiment were measured separately for leaves and stems. Dry weight was measured after  
 194 heating by an electric oven at 105°C for 24 hours. Approximately 2 mg of dried sample was  
 195 ground using a mortar and pestle and elemental carbon content analyzed using a CHNS analyzer  
 196 (Parkin Elmer Co. Ltd., 2400II) in CHN mode to estimate eelgrass biomass.

197

## 198 2.2. Evaluation of coefficients of NEP model

199 Photon flux density and water temperature were measured every 10 minutes. The 10-minute  
 200 data were converted to 1-hour interval data. Nitrogen and phosphorus could limit eelgrass  
 201 respiration and photosynthesis when sediment water NH<sub>4</sub><sup>+</sup>, NO<sub>3</sub><sup>-</sup> + NO<sub>2</sub><sup>-</sup> and PO<sub>4</sub><sup>3-</sup>  
 202 concentrations are lower than 0.1, 0.5 and 0.03 μM, respectively (Lee et al., 2007). We confirmed  
 203 that nitrogen and phosphorus concentrations were sufficient and didn't limit the eelgrass  
 204 respiration and photosynthesis (Table 2). Therefore, in this study, we decided to apply Eq. (1) for  
 205 modelling Net Ecosystem Production by eelgrass (NEP) taking into account photon flux density  
 206 and water temperature. A Jassby type equation and Arrhenius equation were applied to simulate  
 207 photosynthesis related to photon flux density and water temperature (Staeher et al., 2011; Beca-  
 208 Carretero et al., 2018; Burkholz et al., 2019), where NEPR refers to Net Ecosystem Production  
 209 due to Respiration by eelgrass and NEPP to Net Ecosystem Production due to Photosynthesis by  
 210 eelgrass:

$$\begin{aligned} \frac{d}{dt}(\text{DIC}) = \Delta\text{DIC} &= R_A \exp\left(-\frac{E_{aR}}{T_w R}\right) - P_\psi \tanh\left(\frac{\alpha_\psi I}{P_\psi}\right) R_P \exp\left(-\frac{E_{aP}}{T_w R}\right) \\ &= -\text{NEP} = \text{NEPR} - \text{NEPP} \end{aligned} \quad (1)$$

211 where, DIC μmol L<sup>-1</sup> is the dissolved inorganic carbon, R<sub>A</sub> μmol kg<sup>-1</sup> h<sup>-1</sup> is the parameter for  
 212 respiration, E<sub>aR</sub> m<sup>2</sup> kg s<sup>-2</sup> is the activation energy for respiration, T<sub>w</sub> K is the water temperature,  
 213 R m<sup>2</sup> kg s<sup>-2</sup> K<sup>-1</sup> is the Boltzmann constant (1.380649 x 10<sup>-23</sup>), P<sub>ψ</sub> μmol kg<sup>-1</sup> h<sup>-1</sup> and α<sub>ψ</sub> m<sup>2</sup> s kg<sup>-1</sup>  
 214 h<sup>-1</sup> are the parameters for photosynthesis, I μmol m<sup>-2</sup> s<sup>-1</sup> is the photon flux density, R<sub>P</sub> is the  
 215 parameter for photosynthesis, E<sub>aP</sub> m<sup>2</sup> kg s<sup>-2</sup> is the activation energy for photosynthesis.

216 Firstly, the parameters for the respiration term in Eq. (1), R<sub>A</sub> μmol kg<sup>-1</sup> h<sup>-1</sup> and E<sub>aR</sub>, were  
 217 obtained using the fact that photosynthesis activity is negligible from sunset to sunrise when  
 218 photon flux density is zero. We calculated ΔDIC under three water temperatures: 12 °C, 20 °C

219 and 24 °C in order to evaluate the effect of the change in water temperature on eelgrass respiration  
220 in dark conditions. Secondly, the parameters for photosynthesis was obtained by considering  
221 photon flux density and using the  $R_A$  and  $E_{aR}$  for NEPR. Thirdly, we proposed an eelgrass Seasonal  
222 Net Ecosystem Production (SNEP) model using the photon flux density duration recorded in the  
223 field. Finally, we applied the SNEP model to estimate changes in DIC due to eelgrass in Komuke  
224 Lagoon.

225

### 226 3. Results

#### 227 3.1. Biological characteristics of eelgrass

228 The dry weight and biomass (carbon content) of eelgrass used in the laboratory experiment are  
229 shown in Table 1 and nutrient concentrations in the lagoon water are shown in Table 2. The  
230 biomass shown in Table 1 was based on the carbon content per unit leaf area calculated from the  
231 elemental carbon content and measured size of eelgrass. It should be noted that one data point  
232 was not available due to a measurement error. Mean leaf biomass was about 288 g C using the  
233 leaf area of both sides of the leaf  $m^2$ . Although the concentration of  $NO_3$ -N,  $NO_2$ -N,  $NH_4$ -N, and  
234  $PO_4$ -P decreased during the experiment, photosynthetic rates were not limited by nutrients  
235 because concentrations remained sufficiently high (Lee et al., 2007).

236

#### 237 3.2. Thermal effect on NEP

238 Partial pressures of carbon dioxide in water ( $fCO_2$ ) started increasing at 8:00 pm on the 25<sup>th</sup> of  
239 June, and  $fCO_2$  decreased from 5:00 am on the 26<sup>th</sup>. DIC changed in a pattern similar to  $fCO_2$  (Fig.  
240 3). In contrast to the eelgrass experiments, in the control tank, DIC was almost constant, which  
241 suggests that water column photosynthesis and respiration due to organisms other than eelgrass,  
242 such as phytoplankton, were negligible in terms of changes in DIC. Also, since TA changed only  
243 slightly, we found that the eelgrass predominantly affected DIC rather than TA. The maximum  
244 photon flux density occurred at 11:00 am on the 26<sup>th</sup>, when water temperature had increased from  
245 12 to 27 °C.  $\Delta DIC$  ( $=-NEP$ )  $\mu mol kg^{-1} h^{-1}$  was negative from 5:00 am on the 25<sup>th</sup> to 5:00 pm on  
246 the 26<sup>th</sup>, which demonstrated positive net ecosystem production (Fig. 3f).

247 When NEP was plotted against photon flux density, NEP values showed different tendencies  
248 below and above 250  $\mu mol m^{-2} s^{-1}$  (Fig. 4). Red circles in Fig. 4 indicate 5 samples from 7:00 am  
249 to 11:00 am on the 26<sup>th</sup>, and green circles indicate 5 samples from 0:00 pm to 4:00 pm on the 26<sup>th</sup>.  
250 Red and green circle samples were sampled under mean water temperature of 16 °C and 25 °C,  
251 respectively. Therefore, it is noted that mean water temperature is a key factor controlling the

252 tendencies of NEP, which suggests the development of a NEPP parameterization needs to include  
253 the effect of water temperature in Eq. (1).

254

### 255 3.3. Estimation of coefficients of NEPR

256 Values for  $R_A$  and  $E_{aR}$  were obtained by assuming that  $\Delta DIC$  represents NEPR from 7:00 pm  
257 of the 25<sup>th</sup> to 3:00 am of the 26<sup>th</sup> and from 6:00 pm to 7:00 pm of the 26<sup>th</sup> when photosynthetic  
258 activity is negligible (Fig. 5). It should be noted that only data with the condition  $\Delta DIC > 0$  was  
259 applied because the respiration term, NEPR, should be higher than zero. Since  $\Delta DIC$  from the  
260 25<sup>th</sup> to 26<sup>th</sup> of June in 2018 was obtained when the water temperature was about 20 °C, we  
261 conducted separate laboratory experiments on the 10<sup>th</sup> of September 2018 with different water  
262 temperature conditions. Finally, 9 validated samples were obtained, in which a significant  
263 difference was confirmed to exist at the 5 % level using a Kruskal Wallis test. Although there are  
264 some fluctuations evident in Figure 5, parameters for respiration could be obtained based on  
265 strong relationships with water temperature:  $R_A = 1.04 \times 10^{17} \mu\text{mol kg}^{-1} \text{h}^{-1}$  and  $E_{aR} = 1.52 \times 10^{-19}$   
266  $\text{m}^2 \text{kg s}^{-2}$  with  $R^2 = 0.68$ .

267

### 268 3.4. Estimation of coefficients of NEPP

269 By applying  $R_A = 1.04 \times 10^{17} \mu\text{mol kg}^{-1} \text{h}^{-1}$  and  $E_{aR} = 1.52 \times 10^{-19} \text{m}^2 \text{kg s}^{-2}$  into NEPR of Eq. (1),  
270 NEPP was obtained using Eq. (2):

$$\text{NEPP} = -\Delta\text{DIC} + \text{NEPR} = -\Delta\text{DIC} + R_A \exp\left(-\frac{E_{aR}}{T_w R}\right) \quad (2)$$

271 and the relationship between photon flux density and NEPP is shown in Fig. 6.

272 To investigate thermal dependence of eelgrass photosynthesis, a value that ignores thermal  
273 effects,  $\text{NEPP}_{noT}$ , was plotted against photon flux density using Eq. (3) (solid lines in Fig. 6):

$$\text{NEPP}_{noT} = P_\psi \tanh\left(\frac{\alpha_\psi I}{P_\psi}\right) \quad (3)$$

274 when the parameters are given as  $P_{\psi noT} = 21.5 \mu\text{mol kg}^{-1} \text{h}^{-1}$  and  $\alpha_{\psi noT} = 21.5/200 \text{m}^2 \text{s kg}^{-1} \text{h}^{-1}$ ,  
275 comparison between NEPP and  $\text{NEPP}_{noT}$  revealed a large difference in the tendencies between  
276 afternoon (green) and morning (red) conditions; red circles represented water samples from  
277 temperatures ranging from 12 to 20 °C, and green circles from 22 to 27 °C. The higher the water  
278 temperature, the larger the NEPP and vice versa, which is similar to the differences in the  
279 tendencies of NEPR. Therefore, an attempt was made to correct for the effect of temperature on  
280 the parameters for photosynthetic activity,  $R_P$  and  $E_{aP}$ , using  $\text{NEPP} / \text{NEPP}_{noT}$ , (Fig. 7):

$$\frac{\text{NEPP}}{\text{NEPP}_{noT}} = R_P \exp\left(-\frac{E_{aP}}{T_w R}\right) \quad (4)$$

281 where  $R_P=2.30 \times 10^7$  and  $E_{aP}=0.69 \times 10^{-19} \text{ m}^2 \text{ kg s}^{-2}$  were obtained with good agreement ( $R^2=0.92$ ).  
 282 To test whether water temperature and NEPP /  $\text{NEPP}_{noT}$  originate from the same distribution, we  
 283 applied a Kruskal Wallis test at the 5 % level. Significant differences were confirmed between  
 284 water temperature and NEPP /  $\text{NEPP}_{noT}$ , thus we obtained parameters for Eq. (1) as  $R_A=1.04 \times$   
 285  $10^{17} \text{ } \mu\text{mol kg}^{-1} \text{ h}^{-1}$ ,  $E_{aR}=1.52 \times 10^{-19} \text{ m}^2 \text{ kg s}^{-2}$ ,  $P_\psi=21.5 \text{ } \mu\text{mol kg}^{-1} \text{ h}^{-1}$ ,  $\alpha_\psi=21.5/200 \text{ m}^2 \text{ s kg}^{-1} \text{ h}^{-1}$ ,  
 286  $R_P=2.30 \times 10^7$  and  $E_{aP}=0.69 \times 10^{-19} \text{ m}^2 \text{ kg s}^{-2}$ .

287

### 288 3.5. Proposal of the SNEP model

289 Eq. (1) can not only be applied to analyze local-scale NEP, for example though coupling with  
 290 a three-dimensional hydrodynamic model, but it can also be applied to estimate the long-term  
 291 (seasonal) change in DIC in enclosed waterbodies. To this end, we propose a method to estimate  
 292 Seasonal Net Ecosystem Production (SNEP) by adapting Eq. (1). To estimate SNEP, it is  
 293 necessary to include the hourly change in DIC (Dennison et al., 1982; Dennison et al., 1985), and  
 294 SNEP is defined by integrating Eq. (1) for one day:

$$\begin{aligned} \text{SNEP} = & -R_A \frac{1}{t_{1day}} \int \exp\left(-\frac{E_{aR}}{T_w R}\right) dt \\ & + P_\psi \frac{1}{t_{1day}} R_P \int \tanh\left(\frac{\alpha_\psi \beta_I I_S}{P_\psi}\right) \exp\left(-\frac{E_{aP}}{T_w R}\right) dt \end{aligned} \quad (5)$$

295 where,  $t_{1day}$  is the integration period (= 24 h),  $\beta_I$  is the effectiveness coefficient (0: no photon flux  
 296 density to 1: maximum photon flux density), and  $I_S$  is the photon flux density at water surface.

297 By assuming that water temperature changes sinusoidally:

$$T_w = T_m + T_h = T_m + T_{h0} \sin\left(\frac{2\pi}{24}t - \frac{\pi}{2}\right) \quad (6)$$

Eq. (5) can be simplified to:

$$\text{SNEP} \approx -R_A \exp\left(-\frac{E_{aR}}{T_m R}\right) \gamma_R + P_\psi \exp\left(-\frac{E_{aP}}{T_m R}\right) \gamma_P \quad (7)$$

where

$$\gamma_R = \frac{1}{t_{1day}} \int \exp\left(\frac{E_{aR} T_h}{T_m^2 R}\right) dt \quad (8)$$

$$\gamma_P = \frac{1}{t_{1day}} \int \tanh\left(\frac{\alpha_\psi \beta_I I_S}{P_\psi}\right) \exp\left(\frac{E_{aP} T_h}{T_m^2 R}\right) dt \quad (9)$$

298 where,  $T_m$  Celsius degree is the daily mean water temperature,  $T_h = T_w - T_m$ ,  $T_{h0}$  is the amplitude  
 299 of water temperature in a day, and  $t$  h is the time from 0 to 24 h. It should be noted that it is  
 300 necessary to include the influence of topographical and tidal effects on a specific location because  
 301 the photon flux density reaching the canopy may change significantly due to changes in  
 302 bathymetry and tides. These effects can be included by changing the value of  $\beta_I$ , which is the  
 303 parameter for attenuation of photon flux density and is a function of the extinction coefficient for  
 304 light attenuation (Dennison et al., 1986).

305 To estimate and project dissolved oxygen (DO) over the bottom in an enclosed bay, Nakayama  
 306 et al., (2010) demonstrated the suitability of a conceptual DO model by taking into account  
 307 residence time between the inside of the bay and the outer ocean (Okada and Nakayama, 2007;  
 308 Okada et al., 2011; Sato et al., 2012). This study thus makes an attempt to propose a SNEP model  
 309 to estimate DIC using the SNEP approach and accounting for water exchange (Fig. 8):

$$V_0 \frac{d}{dt} (DIC_S) = -V_0 \text{SNEP} - (Q_E + Q_R) DIC_S + Q_E DIC_{out} + Q_R DIC_R \quad (10)$$

310 where,  $DIC_S \mu\text{mol kg}^{-1}$  is the monthly mean DIC,  $V_0 \text{m}^3$  is the volume of the lagoon,  $Q_E \text{m}^3 \text{s}^{-1}$  is  
 311 the exchange flux between a lake and the ocean,  $Q_R \text{m}^3 \text{s}^{-1}$  is the river discharge,  $DIC_R \mu\text{mol kg}^{-1}$   
 312 is DIC of a river, and  $DIC_{out} \mu\text{mol kg}^{-1}$  is the typical DIC concentration of the ocean. We note that  
 313 this model assumes the net atmospheric exchange of  $\text{CO}_2$  over the period of the calculation is  
 314 negligible, which is supported by estimates from in situ  $f\text{CO}_2$  values.

315 By assuming a steady state in Eq. (10) (i.e. the left term is zero), the change in  $DIC_S$  can be  
 316 obtained as:

$$\Delta DIC_S = DIC_{stable} - DIC_S = t_S \text{SNEP} \quad (11)$$

$$t_S = \frac{V_0}{Q_E + Q_R} \quad (12)$$

$$DIC_{stable} = \frac{Q_E DIC_{out} + Q_R DIC_R}{Q_E + Q_R} \quad (13)$$

317 where,  $\Delta DIC_S \mu\text{mol kg}^{-1}$  is the change in DIC with NEP,  $DIC_{stable} \mu\text{mol kg}^{-1}$  is DIC in a steady  
 318 state without NEP ( $\text{NEP} = 0$ ), and  $t_S$  h is the residence time of the target domain. In other words,  
 319 if we obtain residence time,  $t_S$ , and SNEP, the change in DIC due to eelgrass can be estimated  
 320 using Eq. (11), and used as a measure of system scale carbon uptake.

321

#### 322 4. Discussion

323 In this study, we obtained parameters needed to simulate the response of photosynthesis to  
324 photon flux density and water temperature based on a Jassby type P-I equation and an Arrhenius  
325 equation (Staehr et al., 2011; Beca-Carretero et al., 2018; Burkholz et al., 2019). Lee et al. (2007)  
326 found that laboratory experiments tend to underestimate saturation irradiance because of the usage  
327 of leaf segments. Since we did not remove the roots in our laboratory experiments, the saturation  
328 irradiance was estimated as  $200 \mu\text{mol m}^{-2} \text{s}^{-1}$  by  $P_{\psi \text{ noT}} / \alpha_{\psi \text{ noT}}$ , where  $P_{\psi \text{ noT}}=21.5 \mu\text{mol kg}^{-1} \text{h}^{-1}$   
329 and  $\alpha_{\psi \text{ noT}}=21.5/200 \text{ m}^2 \text{s kg}^{-1} \text{h}^{-1}$ . The value is larger than the average level of saturation irradiance  
330 for leaf segments of *Zostera marina*,  $116 \mu\text{mol m}^{-2} \text{s}^{-1}$ , while the average value of saturation  
331 irradiance for whole plant is  $450 \mu\text{mol m}^{-2} \text{s}^{-1}$  (Lee et al., 2007).

332 The rate of change in NEP due to photosynthesis and respiration has been shown to increase  
333 with increasing water temperature (Dennison, 1987; Orth et al., 1986; Phillips et al., 1983;  
334 Bulthuis, 1987; Setchell, 1929). To understand thermal dependencies, NEPP, NEPR and NEP  
335 were computed by changing water temperatures from  $5 \text{ }^\circ\text{C}$  to  $30 \text{ }^\circ\text{C}$  using Eq. (1) (Fig. 9). NEPP  
336 and NEPR increased with the increasing water temperature (Fig. 9a and Fig. 9b). When the photon  
337 flux density was more than about  $250 \mu\text{mol m}^{-2} \text{s}^{-1}$ , NEPP varied from  $8 \mu\text{mol kg}^{-1} \text{h}^{-1}$  to  $34 \mu$   
338  $\text{mol kg}^{-1} \text{h}^{-1}$ , an increase of  $26 \mu\text{mol kg}^{-1} \text{h}^{-1}$  (Fig. 9a). In comparison, NEP under a thermal  
339 increase from  $5$  to  $30 \text{ }^\circ\text{C}$  varied from  $7 \mu\text{mol kg}^{-1} \text{h}^{-1}$  to  $17 \mu\text{mol kg}^{-1} \text{h}^{-1}$ , an increase of  $10 \mu\text{mol}$   
340  $\text{kg}^{-1} \text{h}^{-1}$  (Fig. 9c). Furthermore, when photon flux density was more than  $250 \mu\text{mol m}^{-2} \text{s}^{-1}$ , NEP  
341 was almost constant under a thermal increase from  $25$  to  $30 \text{ }^\circ\text{C}$  because the increase in NEPR was  
342 almost equal to the increase in NEPP (Fig. 9c). Lee et al. (2007) revealed that the average value  
343 of optimal temperature of *Zostera marina* is about  $15 \text{ }^\circ\text{C}$  for growth and  $23 \text{ }^\circ\text{C}$  for photosynthesis,  
344 which is in good agreement with our study with optimal temperatures of about  $25 \text{ }^\circ\text{C}$  for  
345 photosynthesis.

346 We applied the SNEP model to Komuke Lagoon to explore the applicability for the evaluation  
347 of seasonal changes in DIC. We referred to the field observations which were conducted in  
348 Komuke Lagoon in May 2013 (Tada et al., 2018) and August 2018. May and August were chosen  
349 as target months in order to clarify the seasonal effect of the difference in water temperature  
350 between spring and summer. Firstly,  $\gamma_R$  and  $\gamma_P$  for SNEP were estimated from Eqs. (8) and (9)  
351 by giving 5 different  $\beta_I$ : 100 %, 75%, 50 %, 25 % and 10 % (Table 3). This showed that  $\gamma_P$   
352 varied greatly with the change in  $\beta_I$ . In contrast to  $\beta_I$ , the difference in photon flux density  
353 between May and August was negligible and the values for  $\gamma_P$  were the same between the two  
354 seasons. Since eelgrass meadows exist from the bottom to a water depth of about 1.0 m in Komuke

355 Lagoon, and the extinction coefficient was about  $2.0 \text{ m}^{-1}$  including the effect of turbidity with a  
356 mean water depth of 2.0 m,  $\beta_I$  was obtained as 25 % using Eq. (14):

$$\beta_I = \frac{1}{h_m} \int_0^{l_E} \exp[-k_E(h_m - z)] dz \quad (14)$$

357 where,  $h_m$  m is the mean water depth,  $k_E \text{ m}^{-1}$  is the extinction coefficient, and  $l_E$  m is the deflected  
358 vegetation height.

359 SNEP was computed against water temperature,  $T_w$ , from  $\beta_I = 0 \%$  to  $\beta_I = 100 \%$  (Fig. 10).  
360 Although the SNEP did not change much from  $\beta_I = 50 \%$  to  $\beta_I = 100 \%$ , SNEP decreases  
361 greatly from  $\beta_I = 50 \%$  to  $\beta_I = 0 \%$ . When  $\beta_I$  was 25 %, a peak in SNEP appeared at a water  
362 temperature of  $15 \text{ }^\circ\text{C}$  and SNEP became negative when the water temperature was more than  
363  $28 \text{ }^\circ\text{C}$ . Watanabe et al. (2005) demonstrated that optimal temperature for *Zostera marina* is  
364  $16.1 \text{ }^\circ\text{C}$  in Akkeshi Bay, which is located close to Komuke Lagoon. This may suggest the practical  
365 applicability of the relatively simple SNEP model for real field environments. Tada et al. (2018)  
366 revealed that DIC at the water surface,  $\text{DIC}_S$ , was smaller than the no eelgrass stable condition,  
367  $\text{DIC}_{stabl}$ , in Komuke Lagoon on the 15<sup>th</sup> of May 2013 using a three-dimensional hydrodynamic  
368 model, which shows  $\Delta\text{DIC}_S = \text{DIC}_{stabl} - \text{DIC}_S = 325 \text{ } \mu\text{ mol kg}^{-1}$  (Table 4). The residence time of  
369 Komuke Lagoon was  $t_S = 110 \text{ h}$  and the mean water temperature was  $7.1 \text{ }^\circ\text{C}$ . Since SNEP is  $2.82$   
370  $\mu\text{ mol kg}^{-1} \text{ h}^{-1}$  from Fig. 10,  $t_S$  SNEP can be obtained as  $310 \text{ } \mu\text{ mol kg}^{-1}$ . Therefore, the estimated  
371  $t_S$  SNEP =  $310 \text{ } \mu\text{ mol kg}^{-1}$  approximately agreed with  $\Delta\text{DIC}_S = 325 \text{ } \mu\text{ mol kg}^{-1}$ , which suggests  
372 the applicability of the SNEP model to an enclosed waterbody, when the residence time is known.

373 In addition to the estimation of  $t_S$  SNEP in May 2013, we conducted water sampling at the  
374 water surface in Komuke Lagoon and measured water temperature, salinity and DIC in 2018 in  
375 order to investigate the applicability of the SNEP model Eq. (11) (sampling stations are shown in  
376 Fig. 1). It should be noted that we found no significant differences in water quality and flow fields  
377 between 2013 and 2018 since Komuke Lagoon has a very narrow inlet and the Okhotsk Sea  
378 provides stable periodic annual changes in water quality. The mean water temperature was  $23.5 \text{ }^\circ\text{C}$ ,  
379 which corresponds to  $\text{SNEP} = 2.23 \text{ } \mu\text{ mol kg}^{-1} \text{ h}^{-1}$  using  $\beta_I = 25 \%$  from Fig. 10 (Table 4). As the  
380 residence time is about 110 h,  $t_S$  SNEP was found to be  $245 \text{ } \mu\text{ mol kg}^{-1}$ . Using the low-salinity  
381 endmember of rivers and the high-salinity endmember of the ocean,  $\Delta\text{DIC}_S$  was estimated as  $255$   
382  $\mu\text{ mol kg}^{-1}$  from field observations following Zeebe et al. (2001). Again, the estimated  $t_S$  SNEP =  
383  $245 \text{ } \mu\text{ mol kg}^{-1}$  agreed well with  $\Delta\text{DIC}_S = 255 \text{ } \mu\text{ mol kg}^{-1}$  from the field observations. The proposed  
384 SNEP model is specific to enclosed or semi-enclosed waterbodies and not for suitable for the  
385 open ocean because of the requirement to evaluate residence times. Since eelgrass appears to be

386 adapted to calm conditions, and there is the possibility to obtain residence times accurately for  
387 these waterbodies, this suggests the SNEP model can be useful to improve predictions of carbon  
388 capture and storage by eelgrass populations in protected waters.

389

## 390 5. Conclusion

391 Aiming to understand the NEP of eelgrass in Komuke Lagoon, which is located in the east of  
392 Hokkaido, parameters for NEPR were obtained as  $R_A=1.04 \times 10^{17} \mu \text{ mol kg}^{-1} \text{ h}^{-1}$  and  $E_{aR}=1.52 \times$   
393  $10^{-19} \text{ m}^2 \text{ kg s}^{-2}$  using the hourly change in DIC without photon flux density in laboratory  
394 experiments. The photosynthetic activity of eelgrass was confirmed to be affected by water  
395 temperature from laboratory experiments, and parameters for NEPP were obtained as  $P_{\psi}=21.5 \mu$   
396  $\text{mol kg}^{-1} \text{ h}^{-1}$ ,  $\alpha_{\psi}=21.5/200 \text{ m}^2 \text{ s kg}^{-1} \text{ h}^{-1}$ ,  $R_p=2.30 \times 10^7$  and  $E_{aP}=0.69 \times 10^{-19} \text{ m}^2 \text{ kg s}^{-2}$ . The SNEP  
397 model was proposed, in which the seasonal change in DIC,  $\Delta \text{DIC}_S$ , can be estimated as  $t_S$  SNEP  
398 by using the residence time,  $t_S$ . The SNEP model was applied to two sets of field observations  
399 from Komuke Lagoon, May 2013 and August 2018, and the estimated seasonal change in DIC,  $t_S$   
400 SNEP, was confirmed to agree with  $\Delta \text{DIC}_S$  from field observations. In other words, the seasonal  
401 change in NEP can be obtained as  $\Delta \text{DIC}_S / t_S$  using the residence time,  $t_S$ , and the seasonal change  
402 in DIC,  $\Delta \text{DIC}_S$ , from endmember analysis using field observations. Since the development and  
403 implementation of mitigation measures against global warming is an urgent issue, the proposed  
404 SNEP model in this study may be applied to assist efforts to enhance effective capture and storage  
405 of carbon dioxide through seagrass restoration. Also, the SNEP model may be useful for assessing  
406 changes due to climate change, e.g. as a screening tool to investigate whether the warming trend  
407 improves net productivity or not with limited information.

408

409

410

411



412 Acknowledgments

413 This work was supported by the Japan Society for the Promotion of Science under grant

414 18H01545 and 18KK0119.

415

416

417 References

- 418 1) IPCC, 2014. Climate Change 2014: Synthesis Report. Contribution of Working Groups I, II  
419 and III to the Fifth Assessment Report of the Intergovernmental Panel on Climate Change  
420 [Core Writing Team, R.K. Pachauri and L.A. Meyer (eds.)]. IPCC, Geneva, Switzerland, 151  
421 pp.
- 422 2) Adams, M. P., Hovey, R. K., Hipsey, M. R., Bruce, L. C., Ghisalberti, M., Lowe, R. J., Gruber,  
423 R. K., Ruiz-Montoya, L., Maxwell, P. S., Callaghan, D. P., Kendrick, G. A., O'Brien, K. R.,  
424 2016. Feedback between sediment and light for seagrass: Where is it important? *Limnol.*  
425 *Oceanogr.* 61, 1937-1955.
- 426 3) Beca-Carretero, P., Olesen, B., Marba, N., Krause-Jensen, D., 2018. Response to  
427 experimental warming in northern eelgrass populations: comparison across a range of  
428 temperature adaptations. *Mar. Ecol. Prog. Ser.* 589, 59–72.
- 429 4) Beer, S., Rehnberg, J., 1997. The acquisition of inorganic carbon by the seagrass *Zostera*  
430 *marina*. *Aquat. Bot.* 56, 277–283.
- 431 5) Biebl, R., McRoy, C.P., 1971. Plasmatic resistance and rate of respiration and photosynthesis  
432 of *Zostera marina* at different salinities and temperatures. *Mar. Biol.* 8, 48–56.
- 433 6) Borum, J., 1985. Development of epiphytic communities on eelgrass (*Zostera marina*) along  
434 a nutrient gradient in a Danish estuary. *Mar. Biol.* 87, 211–218.
- 435 7) Boström, C., Roos, C., Rönnerberg, O., 2004. Shoot morphometry and production dynamics  
436 of eelgrass in the northern Baltic Sea. *Aquat. Bot.* 79, 145–161.
- 437 8) Bulthuis, D.A., 1987. Effects of temperature on photosynthesis and growth of seagrasses.  
438 *Aquat. Bot.* 27, 27–40.
- 439 9) Burkholder, J.M., Glasgow Jr., H.B., Cooke, J.E., 1994. Comparative effects of water-  
440 column nitrate enrichment on eelgrass *Zostera marina*, shoalgrass *Halodule wrightii*, and  
441 widgeongrass *Ruppia maritima*. *Mar. Ecol. Prog. Ser.* 105, 121–138.
- 442 10) Burkholder, J.M., Mason, K.M., Glasgow Jr., H.B., 1992. Water-column nitrate enrichment  
443 promotes decline of eelgrass *Zostera marina*: evidence from seasonal mesocosm  
444 experiments. *Mar. Ecol. Prog. Ser.* 81, 163–178.
- 445 11) Burkholz, C., Duarte, C.M., Garcias-Bonet, N., 2019. Thermal dependence of seagrass  
446 ecosystem metabolism in the Red Sea. *Mar. Ecol. Prog. Ser.* 614, 79–90.
- 447 12) Cabello-Pasini, A., Muñoz-Salazar, R., Ward, D.H., 2003. Annual variations of biomass and  
448 photosynthesis in *Zostera marina* at its southern end of distribution in the North Pacific.  
449 *Aquat. Bot.* 76, 31–47.

- 450 13) Capone, D.G., 1982. Nitrogen fixation (acetylene reduction) by rhizosphere sediments of the  
451 eelgrass *Zostera marina*. Mar. Ecol. Prog. Ser. 10, 67–75.
- 452 14) Coleman, V.L., Burkholder, J.M., 1994. Community structure and productivity of epiphytic  
453 microalgae on eelgrass (*Zostera marina* L.) under water-column nitrate enrichment. J. Exp.  
454 Mar. Biol. Ecol. 179, 29–48.
- 455 15) Dennison, W.C., 1987. Effects of light on seagrass photosynthesis, growth and depth  
456 distribution. Aquat. Bot. 27, 15–26.
- 457 16) Dennison, W.C., Alberte, R.S., 1982. Photosynthetic responses of *Zostera marina* L.  
458 (eelgrass) to in situ manipulations of light intensity. Oecologia 55, 137–144.
- 459 17) Dennison, W.C., Alberte, R.S., 1985. Role of daily light period in the depth distribution of  
460 *Zostera marina* (eelgrass). Mar. Ecol. Prog. Ser. 25, 51–61.
- 461 18) Dennison, W.C., Alberte, R.S., 1986. Photoadaptation and growth of *Zostera marina* L.  
462 (eelgrass) transplants along a depth gradient. J. Exp. Mar. Biol. Ecol. 98, 265–282.
- 463 19) Dennison, W.C., Aller, R.C., Alberte, R.S., 1987. Sediment ammonium availability and  
464 eelgrass (*Zostera marina*) growth. Mar. Biol. 94, 469–477.
- 465 20) Dennison, W.C., Orth, R.J., Moore, K.A., Stevenson, J.C., Carter, V., Kollar, S., Bergstrom,  
466 P.W., Batiuk, R.A., 1993. Assessing water quality with submersed aquatic vegetation.  
467 Bioscience 43, 86–94.
- 468 21) Drew, E.A., 1979. Physiological aspects of primary production in seagrasses. Aquat. Bot. 7,  
469 139–150.
- 470 22) Duarte, C.M., Losada, I.J., Hendriks, I.E., Mazarrasa, I., and Marbà, N., 2013. The role of  
471 coastal plant communities for climate change mitigation and adaptation. Nature Climate  
472 Change, 3(11), 961.
- 473 23) Evans, A.S., Webb, K.L., Penhale, P.A., 1986. Photosynthetic temperature acclimation in two  
474 coexisting seagrasses, *Zostera marina* L. and *Ruppia maritima* L. Aquat. Bot. 24, 185–197.
- 475 24) Fourqurean J.W, Duarte, C.M., Kennedy H., Marbà, N., Holmer, M., Mateo, M.A.,  
476 Apostolaki, E.T., Kendrick, G.A., Krause-Jensen, D., McGlathery, K.J., Serrano, O., 2012.  
477 Seagrass ecosystems as a globally significant carbon stock. Nat. Geosci. 5, 505–509.
- 478 25) Goodman, J.L., Moore, K.A., Dennison, W.C., 1995. Photosynthetic responses of eelgrass  
479 (*Zostera marina* L.) to light and sediment sulfide in a shallow barrier island lagoon. Aquat.  
480 Bot. 50, 37–47.
- 481 26) Holmer, M., Bondgaard, E.J., 2001. Photosynthetic and growth response of eelgrass to low  
482 oxygen and high sulfide concentrations during hypoxic events. Aquat. Bot. 70, 29–38.

- 483 27) Ibarra-Obando, S.E., Huerta-Tamayo, R., 1987. Blade production of *Zostera marina* L.  
484 during the summer-autumn period on the pacific coast of Mexico. *Aquat. Bot.* 28, 301–315.
- 485 28) Iizumi, H., Hattori, A., 1982. Growth and organic production of eelgrass (*Zostera marina* L.)  
486 in temperate waters of the Pacific coast of Japan. III. The kinetics of nitrogen uptake. *Aquat.*  
487 *Bot.* 12, 245–256.
- 488 29) Iizumi, H., Hattori, A., McRoy, C.P., 1982. Ammonium regeneration and assimilation in  
489 eelgrass (*Zostera marina*) beds. *Mar. Biol.* 66, 59–65.
- 490 30) Jørgensen, B.B., 1982. Mineralization of organic matter in the sea bed—the role of sulphate  
491 reduction. *Nature* 296, 643–645.
- 492 31) Kennedy, H., Beggins, J., Duarte, C.M., et al., 2010. Seagrass sediments as a global carbon  
493 sink: isotopic constraints. *Glob. Biogeochem. Cy.* 24:GB4026.
- 494 32) Koch, E.W., Beer, S., 1996. Tides, light and the distribution of *Zostera marina* in Long Island  
495 Sound, USA. *Aquat. Bot.* 53, 97–107.
- 496 33) Lee, K.-S., Park, S.R., Kim, J.-B., 2005. Production dynamics of the eelgrass, *Zostera marina*  
497 in two bay systems on the south coast of the Korean peninsula. *Mar. Biol.* 15.0, 1091–1108.
- 498 34) Lee, K.S., Park, S.R., Kim, Y.K., 2007. Effects of irradiance, temperature, and nutrients on  
499 growth dynamics of seagrasses: A review. *J. Exp. Mar. Biol. Ecol.* 350, 144–175.
- 500 35) Lee, S.Y., Kim, J.B., Lee, S.M., 2006. Temporal dynamics of subtidal *Zostera marina* and  
501 intertidal *Zostera japonica* on the southern coast of Korea. *Mar. Ecol.* 27, 133–144.
- 502 36) Macreadie, P.I., Anton, A., Raven, J.A., Beaumont, N., Connolly, M., Friess, D.A., ... Duarte,  
503 C.M., 2019. The future of Blue Carbon science, *Nature Communications* volume 10, Article  
504 number: 3998.
- 505 37) Marsh Jr., J.A., Dennison, W.C., Alberte, R.S., 1986. Effects of temperature on  
506 photosynthesis and respiration in eelgrass (*Zostera marina* L.). *J. Exp. Mar. Biol. Ecol.* 101,  
507 257–267.
- 508 38) Martin, S., Castets, M.D., Clavier, J., 2006. Primary production, respiration and calcification  
509 of the temperate free-living coralline alga *Lithothamnion corallioides*. *Aquat. Bot.* 85, 121–  
510 128.
- 511 39) Mazzella, L., Alberte, R.S., 1986. Light adaptation and the role of autotrophic epiphytes in  
512 primary production of the temperate seagrass, *Zostera marina* L. *J. Exp. Mar. Biol. Ecol.*  
513 100, 165–180.
- 514 40) Moore, K.A., Neckles, H.A., Orth, R.J., 1996. *Zostera marina* (eelgrass) growth and survival  
515 along a gradient of nutrients and turbidity in the lower Chesapeake Bay. *Mar. Ecol. Prog. Ser.*

- 516 142, 247–259.
- 517 41) Moore, K.A., Wetzel, R.L., Orth, R.J., 1997. Seasonal pulses of turbidity and their relations  
518 to eelgrass (*Zostera marina* L.) survival in an estuary. *J. Exp. Mar. Biol. Ecol.* 215, 115–134.
- 519 42) Murray, L., Dennison, W.C., Kemp, W.M., 1992. Nitrogen versus phosphorus limitation for  
520 growth of an estuarine population of eelgrass (*Zostera marina* L.). *Aquat. Bot.* 44, 83–100.
- 521 43) Nakayama, K., Nguyen, H.D., Shintani, T., Komai, K., 2016. Reversal of secondary  
522 circulations in a sharp channel bend. *Coas. Eng. J.* 58, 1650002.
- 523 44) Nakayama, K., Sato, T., Shimizu, K., Boegman, L., 2019. Classification of internal solitary  
524 wave breaking over a slope. *Phys. Rev. Fluids.* 4, 014801.
- 525 45) Nakayama, K., Shintani, T., Kokubo, K., Kakinuma, T., Maruya, Y., Komai, K., Okada, T.,  
526 2012. Residual current over a uniform slope due to breaking of internal waves in a two-layer  
527 system. *J. Geophys. Res.* 117, C10002, 1-11.
- 528 46) Nakayama, K., Shintani, T., Shimizu, K., Okada, T., Hinata, H., Komai, K., 2014. Horizontal  
529 and residual circulations driven by wind stress curl in Tokyo Bay. *J. Geophys. Res.* 119,  
530 1977-1992.
- 531 47) Nakayama, K., Sivapalan, M., Sato, C., Furukawa, K., 2010. Stochastic characterization of  
532 the onset of and recovery from hypoxia in Tokyo Bay, Japan: Derived distribution analysis  
533 based on “strong wind” events, *Wat. Resour. Res.* 46, W12532, 1-15.
- 534 48) Nellemann C., Corcoran E., Duarte C.M., Valdes L., DeYoung C., Fonseca L., Grimsditch  
535 G., 2009. Blue Carbon. A Rapid Response Assessment. United Nations Environmental  
536 Programme, GRID-Arendal, Birkeland.
- 537 49) Okada, T., Nakayama, K., 2007. Modeling of dissolved oxygen in an enclosed bay with sill,  
538 *J. Environ. Eng. - ASCE*, 1(1), 104.
- 539 50) Okada, T., Nakayama, K., Takao, T., Furukawa, K., 2011. Influence of freshwater input and  
540 bay reclamation on long-term changes in seawater residence times in Tokyo Bay, Japan,  
541 *Hydrological Processes*, 24, 2694-2702.
- 542 51) Olesen, B., Sand-Jensen, K., 1993. Seasonal acclimatization of eelgrass *Zostera marina*  
543 growth to light. *Mar. Ecol. Prog. Ser.* 94, 91–99.
- 544 52) Orth, R.J., 1977. Effect of nutrient environment on growth of the eelgrass *Zostera marina* in  
545 the Chesapeake Bay, Virginia, USA. *Mar. Biol.* 44, 187–194.
- 546 53) Orth, R.J., Moore, K.A., 1983. Chesapeake Bay: an unprecedented decline in submerged  
547 aquatic vegetation. *Science* 222, 51–53.
- 548 54) Orth, R.J., Moore, K.A., 1986. Seasonal and year-to-year variations in the growth of *Zostera*

- 549 *marina* L. (eelgrass) in the lower Chesapeake Bay. *Aquat. Bot.* 24, 335–341.
- 550 55) Palacios, S.L., Zimmerman, R.C., 2007. Response of eelgrass *Zostera marina* to CO<sub>2</sub>  
551 enrichment: possible impacts of climate change and potential for remediation of coastal  
552 habitats. *Mar. Ecol. Prog. Ser.* 344, 1–13.
- 553 56) Pedersen, M.F., Borum, J., 1992. Nitrogen dynamics of eelgrass *Zostera marina* during a late  
554 summer period of high growth and low nutrient availability. *Mar. Ecol. Prog. Ser.* 80, 65–73.
- 555 57) Pedersen, M.F., Borum, J., 1993. An annual nitrogen budget for a seagrass *Zostera marina*  
556 population. *Mar. Ecol. Prog. Ser.* 101, 169–177.
- 557 58) Penhale, P.A., 1977. Macrophyte-epiphyte biomass and productivity in an eelgrass (*Zostera*  
558 *marina* L.) community. *J. Exp. Mar. Biol. Ecol.* 26, 211–224.
- 559 59) Phillips, R.C., McMillan, C., Bridges, K.W., 1983. Phenology of eelgrass, *Zostera marina*  
560 L., along latitudinal gradients in North America. *Aquat. Bot.* 15, 145–156.
- 561 60) Sand-Jensen, K., 1975. Biomass, net production and growth dynamics in an eelgrass (*Zostera*  
562 *marina* L.) population in Vellerup Vig, Denmark. *Ophelia* 14, 185–201.
- 563 61) Satoh, C., Nakayama, K., Furukawa, K., 2012. Contributions of wind and river effects on  
564 DO concentration in Tokyo Bay, *Estuarine Coast and Shelf Science*, 109, 91-97.
- 565 62) Setchell, W.A., 1929. Morphological and phenological notes on *Zostera marina* L. *Univ. Calif.*  
566 *Publ. Bot.* 14, 389–452.
- 567 63) Sfriso, A., Ghetti, P.F., 1998. Seasonal variation in biomass, morphometric parameters and  
568 production of seagrasses in the lagoon of Venice. *Aquat. Bot.* 61, 207–223.
- 569 64) Shintani, T., Nakayama, K., 2010. An object-oriented approach to environmental fluid  
570 modeling. *The 21st International Symposium on Transport Phenomena*.
- 571 65) Short, F.T., 1987. Effects of sediment nutrients on seagrasses: literature review and  
572 mesocosm experiment. *Aquat. Bot.* 27, 41–57.
- 573 66) Short, F.T., Burdick, D.M., Kaldy, J.E., 1995. Mesocosm experiments quantify the effects of  
574 eutrophication on eelgrass, *Zostera marina*. *Limnol. Oceanogr.* 40, 740–749.
- 575 67) Short, F.T., McRoy, C.P., 1984. Nitrogen uptake by leaves and roots of the seagrass *Zostera*  
576 *marina* L. *Bot. Mar.* 27, 547–555.
- 577 68) Short, F.T., Neckles, H.A., 1999. The effects of global climate change on seagrasses. *Aquat.*  
578 *Bot.* 63, 169–196.
- 579 69) Staehr, P.A., Borum, J., 2011. Seasonal acclimation in metabolism reduces light requirements  
580 of eelgrass (*Zostera marina*). *J. Exp. Mar. Biol. Ecol.* 407, 139–146.
- 581 70) Tada, K., Nakayama, K., Komai, K., Tsai, J.W., Sato, Y., Kuwae, T., 2018. Analysis of

- 582 dissolved inorganic carbon due to seagrass in a stratified flow. J. Japan Soc. Civil Eng., Ser.  
583 B3. 74, 444-449.
- 584 71) Thursby, G.B., Harlin, M.M., 1982. Leaf-root interaction in the uptake of ammonia by  
585 *Zostera marina*. Mar. Biol. 72, 109-112.
- 586 72) Touchette, B.W., 1999. Physiological and developmental responses of eelgrass (*Zostera*  
587 *marina* L.) to increases in water-column nitrate and temperature. Ph.D. Dissertation, North  
588 Carolina State University, Raleigh, NC.
- 589 73) Van Lent, F., Verchuure, J.M., van Veghel, L.J., 1995. Comparative study on populations of  
590 *Zostera marina* L. (eelgrass): in situ nitrogen enrichment and light manipulation. J. Exp. Mar.  
591 Biol. Ecol. 185, 55-76.
- 592 74) Watanabe, M., Nakaoka, M., Mukai, H., 2005. Seasonal variation in vegetative growth and  
593 production of the endemic Japanese seagrass *Zostera asiatica*: a comparison with sympatric  
594 *Zostera marina*. Bot. Mar. 48, 266-273.
- 595 75) Williams, S.L., Ruckelshaus, M.H., 1993. Effects of nitrogen availability and herbivory on  
596 eelgrass (*Zostera marina*) and epiphytes. Ecology 74, 904-918.
- 597 76) Zeebe, R.E., Wolf-Gladrow, D., 2001. Equilibrium. In: CO<sub>2</sub> in Seawater: Equilibrium,  
598 Kinetics, Isotopes. Elsevier, Amsterdam, 1-83.
- 599 77) Zimmerman, R.C., Kohrs, D.G., Steller, D.L., Alberte, R.S., 1997. Impacts of CO<sub>2</sub>  
600 enrichment on productivity and light requirements of eelgrass. Plant Physiol. 115, 599-607.
- 601 78) Zimmerman, R.C., Reguzzoni, J.L., Alberte, R.S., 1995. Eelgrass (*Zostera marina* L.)  
602 transplants in San Francisco Bay: role of light availability on metabolism, growth and  
603 survival. Aquat. Bot. 51, 67-86.
- 604 79) Zimmerman, R.C., Smith, R.D., Alberte, R.S., 1987. Is growth of eelgrass nitrogen limited?  
605 A numerical simulation of the effects of light and nitrogen on the growth dynamics of *Zostera*  
606 *marina*. Mar. Ecol. Prog. Ser. 41, 167-176.
- 607

608 Figure

609

610 Fig. 1 Sampling stations in Komuke Lagoon

611

612 Fig. 2. Schematic diagram of the laboratory experiment tank containing eelgrass

613

614 Fig. 3. Laboratory experiment results from 21:00 on the 25<sup>th</sup> to 19:00 on the 26<sup>th</sup> of June 2018.

615 (a)  $f\text{CO}_2$  with and without eelgrass. (b) DIC with and without eelgrass. (c) TA with and without

616 eelgrass. (d) photon flux density. (e) water temperature. (f)  $\Delta\text{DIC}$ .

617

618 Fig. 4. Photon flux density and NEP.

619

620 Fig. 5. Water temperature and  $\Delta\text{DIC}$ . Solid line is the first term of equation (1).

621

622 Fig. 6. Photon flux density and NEPP by equation (2). Solid line is equation (3).

623

624 Fig. 7. Water temperature and the ratio of NEPP and  $\text{NEPP}_{not}$ . Solid line is equation (4).

625

626 Fig. 8. Schematic diagram of SNEP model.

627

628 Fig. 9. Effect of water temperature on (a) NEPP, (b) NEPR and (c) NEP.

629

630 Fig. 10. Water temperature and DNEP in Komuke Lagoon.

631

632

633



634 Table

635

636 Table 1. Specimens in laboratory experiments.

637

638 Table 2. Nutrient concentrations in experimental water.

639

640 Table 3.  $\gamma_R$  and  $\gamma_P$  in May 2013 and August 2018.

641

642 Table 4. Field observations in Lake Komuke.

643

644

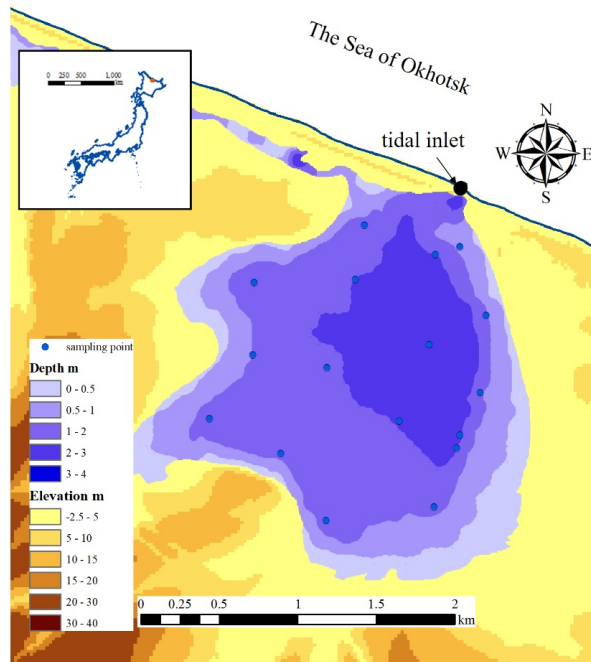
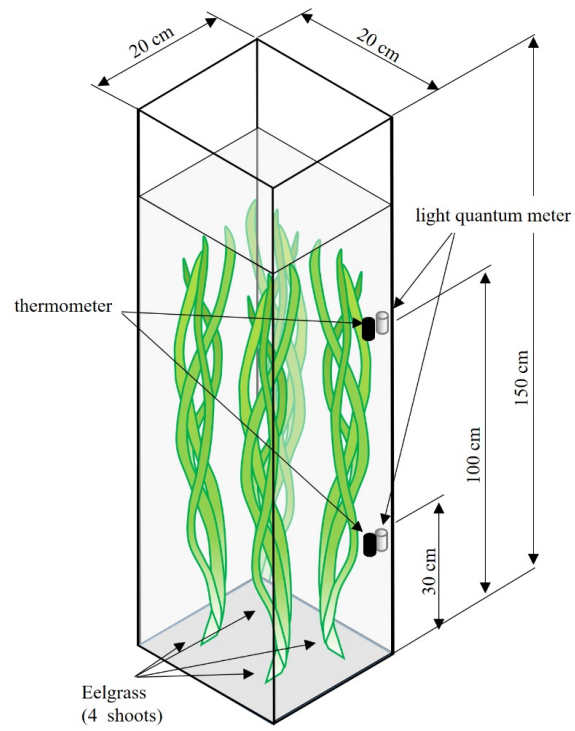


Fig. 1 Sampling stations in Komuke Lagoon

645  
646  
647

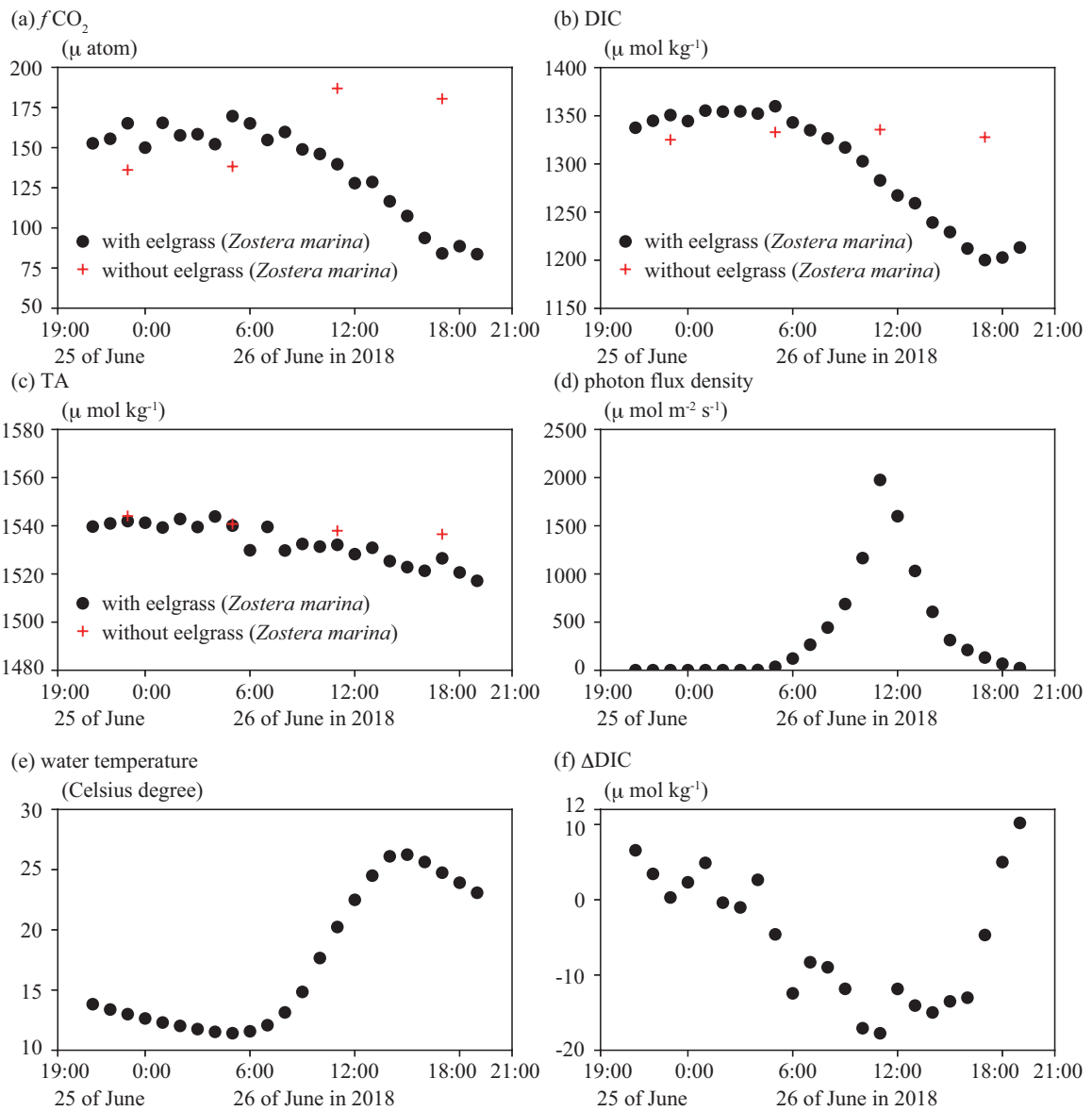


648

649

650

Fig. 2. Schematic diagram of the laboratory experiment tank containing eelgrass



651

652

Fig. 3. Laboratory experiment results from 21:00 on the 25<sup>th</sup> to 19:00 on the 26<sup>th</sup> of June 2018.

653

(a)  $f\text{CO}_2$  with and without eelgrass. (b) DIC with and without

654

eelgrass. (d) photon flux density. (e) water temperature. (f)  $\Delta\text{DIC}$ .

655

656

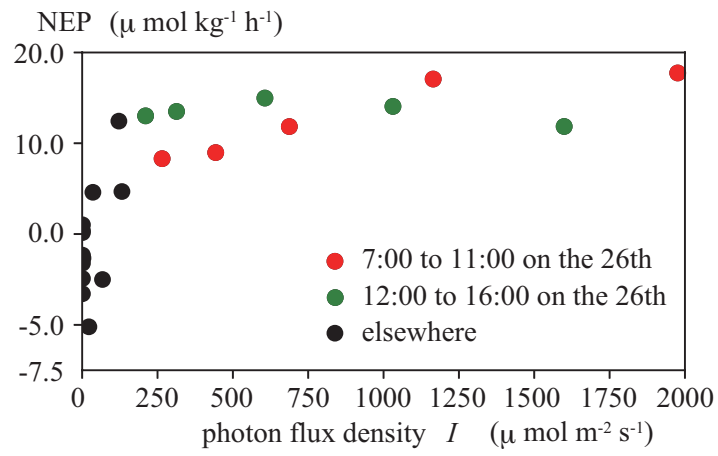


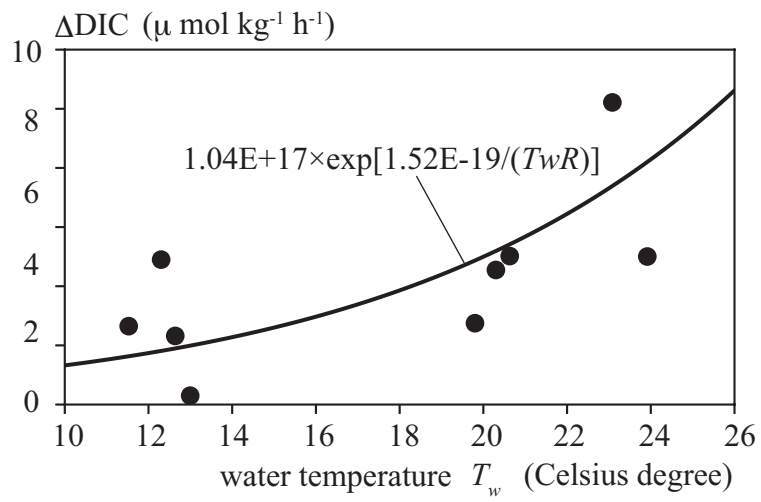
Fig. 4. Photon flux density and NEP.

657

658

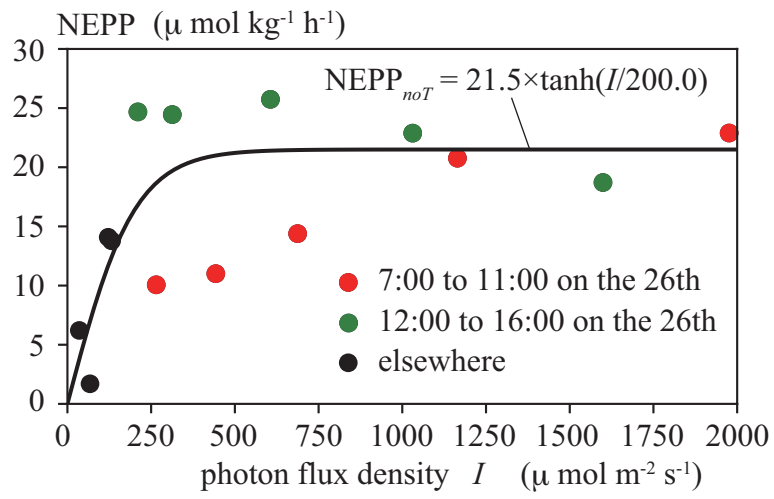
659

660



661  
 662  
 663  
 664

Fig. 5. Water temperature and  $\Delta\text{DIC}$ . Solid line is the first term of equation (1).



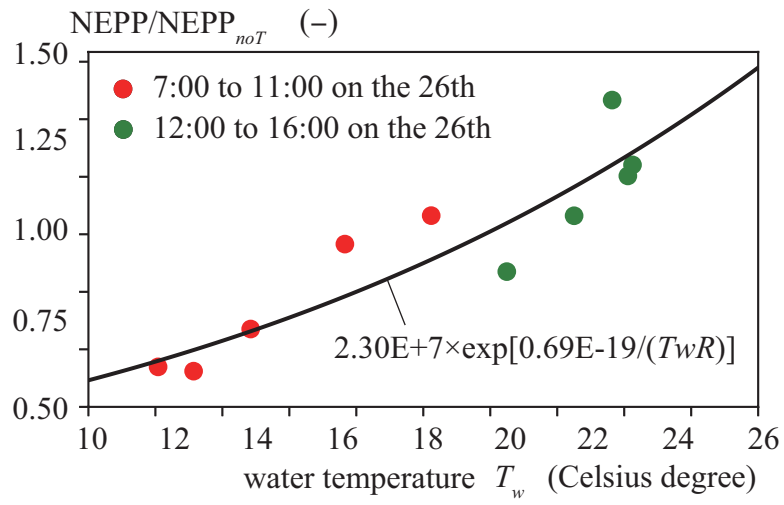
665

666

667

668

Fig. 6. Photon flux density and NEPP by equation (2). Solid line is equation (3).



669

670

Fig. 7. Water temperature and the ratio of NEPP and NEPP<sub>noT</sub>. Solid line is equation (4).

671

672



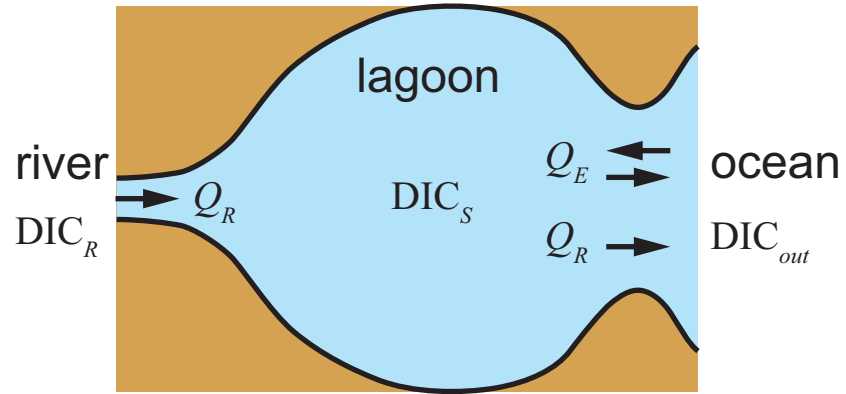


Fig. 8. Schematic diagram of SNEP model.

673

674

675

676

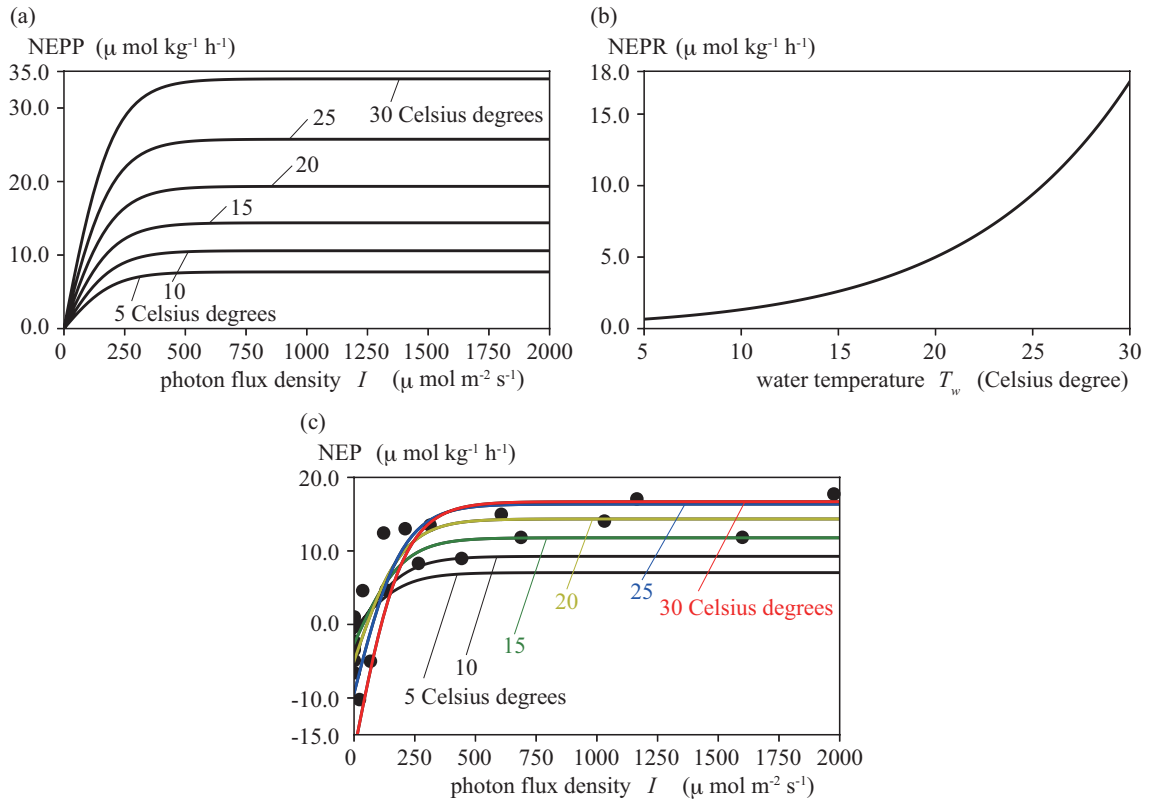


Fig. 9. Effect of water temperature on (a) NEPP, (b) NEPR and (c) NEP.

677  
 678  
 679  
 680

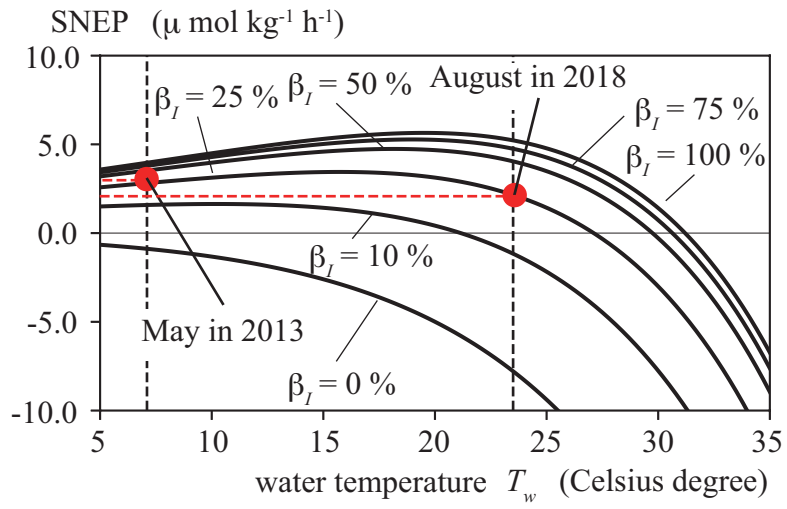


Fig. 10. Water temperature and DNEP in Komuke Lagoon.

681  
 682  
 683  
 684

685

Table 1. Specimens in laboratory experiments.

Eelgrass No.	Dry weight (leaf) (g)	Leaf biomass (g C/m <sup>2</sup> )
1	379.94	253.15
2	419.07	284.27
3	490.96	325.87

686

687

688

Table 2. Nutrient concentrations in experimental water.

Water sample	NO <sub>3</sub> -N ( $\mu$ M)	NO <sub>2</sub> -N ( $\mu$ M)	NH <sub>4</sub> -N ( $\mu$ M)	PO <sub>4</sub> -P ( $\mu$ M)
Before experiment	1.642	0.100	2.127	0.804
After experiment	0.899	0.079	0.671	0.565

689

690

691

Table 3.  $\gamma_R$  and  $\gamma_P$  in May 2013 and August 2018.

$\beta_I$	100%	75%	50%	25%	10%	0%
$\gamma_R$	1.01					
$\gamma_P$ (May in 2013)	0.56	0.54	0.51	0.42	0.28	0
$\gamma_P$ (August in 2018)	0.54	0.52	0.49	0.42	0.28	0
$\gamma_P$ (mean)	0.55	0.53	0.50	0.42	0.28	0

692

693

694

Table 4. Field observations in Lake Komuke.

	Mean water temperature (Celsius degree)	$t_S$ (h)	$\Delta\text{DIC}_S$ ( $\mu\text{ mol kg}^{-1}$ ) from observation	SNEP ( $\mu\text{ mol kg}^{-1}\text{ h}^{-1}$ ) from (7)	$t_S$ SNEP ( $\mu\text{ mol kg}^{-1}$ )
May 2013	7.1	110	325	2.82	310
August 2018	23.5	110	255	2.23	245

695

696

697

698